

Structural and electronic properties of cleaved Si(111) upon room-temperature formation of an interface with Ag

D. Bolmont,* Ping Chen,[†] C. A. Sebenne, and F. Proix

*Laboratoire de Physique des Solides, Associé au Centre National de la Recherche Scientifique,
Université Pierre et Marie Curie, Paris, France*

(Received 31 December 1980)

Photoemission yield spectroscopy, low-energy-electron-diffraction (LEED), and Auger measurements are performed on a set of UHV cleaved silicon (111) surfaces with different bulk dopings as a function of silver coverage Θ . The Ag layers are obtained by evaporation on the substrate kept at room temperature and Θ varies from zero to a few monolayers (ML). It is demonstrated that the interface forms in two steps. First, an ordered layer of silver develops on top of the 2×1 reconstructed silicon which remains unperturbed. The silver layer exhibits a $(\sqrt{7} \times \sqrt{7})R 19.1^\circ$ structure and is completed at about 0.7 ML of Ag. Both the work function and the ionization energy decrease by the same amount, the density of surface states being only slightly perturbed. Then upon further silver deposition, the 1×1 LEED structure of Ag(111) develops on top of the preceding ones which remain observable while new electron states induced by silver metal are added without changing the electronic character of the interface.

I. INTRODUCTION

The wide variety of techniques which have been developed to study solid surfaces during the last two decades are more and more devoted to getting some insight on the microscopic properties which characterize solid-solid interfaces. This can be done during the formation of the interface which therefore must be prepared under ultrahigh vacuum. The development of methods allowing the preparation of a well-controlled substrate and the deposition of a known amount of pure material has made the study of interface formation an attractive subject for the last few years. Among the family of metal-semiconductor interfaces, the system Ag-Si(111) appears quite interesting to correlate the local structure with the electronic properties for several reasons. First, the crystallography and the electronic structure of the clean (111) face of silicon obtained by cleavage under ultrahigh vacuum are fairly well known.¹ Second, the silver silicon interface forms after a deposit which is in the monolayer range [one monolayer (ML) corresponds to one adsorbed atom per substrate surface atom, that is about $7.8 \times 10^{14} \text{ cm}^{-2}$ for Si(111)] and is not changed upon increasing coverage.^{2,3} Third, structural changes at the interface can be thermally induced.³ Fourth, another surface structure of Si(111) characterized by the well known 7×7 low-energy-electron-diffraction (LEED) pattern can be

prepared before silver deposit.

Most of the studies of the Ag-Si(111) interface formation concern the initially clean 7×7 reconstructed Si(111) surface. Several techniques have been employed, either separately or simultaneously, such as LEED, Auger electron spectroscopy, reflection high-energy electron diffraction (RHEED), photoemission spectroscopy, and/or electron energy-loss spectroscopy, by the following different groups after Spiegel⁴ and Bauer and Poppa²: Le Lay *et al.*,^{5,6} Wehking *et al.*,⁷ Housley *et al.*,⁸ Ino and Gotoh,^{9,10} Derrien *et al.*,¹¹ and Gaspard *et al.*¹² Some work concerns also the 2×1 reconstructed Si(111) surface interacting with silver at room temperature; besides some information given in Refs. 3 and 11, a study by McKinley *et al.*¹³ has been fully devoted to this case. The reason why less attention has been paid to the Ag-Si(111) (2×1) system is probably because the growth process is admittedly by a two-dimensional silver film with its (111) plane parallel to the (111) plane of silicon, no specific LEED structure being observed during interface formation.^{3,13} The photoemission measurements show an intermediate behavior which is not the simple addition of silicon and silver states,¹³ around 1 ML silver coverage.¹³ An interesting point comes from Schottky-barrier measurements by Thanailakis¹⁴ and Van Otterloo and De Groot.¹⁵ On *n*-type samples, Schottky-barrier heights (distance between Fermi level and bottom

of the conduction band at the interface) are found between 0.70 and 0.80 eV; the better the cleave, the greater the height. Unfortunately, the effect of the sample doping on the barrier height has not been measured. This would be interesting because the interface position of the Fermi level with respect to the silicon conduction band is the same, within experimental uncertainties, as the surface position obtained for the clean cleaved surface where it moves only slightly (by about 0.15 eV) when the sample doping varies from highly n to highly p .¹ A direct investigation of the density of the localized states during the interface formation correlated with the local structure appeared necessary. In the present paper we describe and discuss the results of a study where the high sensitivity and good energy resolution of photoemission yield spectroscopy are exploited, together with LEED and Auger measurements, to get some insight on the formation of the Si(111) (2×1) -Ag interface at room temperature.

II. EXPERIMENTAL

The experiments are performed in a stainless-steel vacuum chamber shown schematically in Fig. 1. A base pressure of about 1×10^{-10} Torr is obtained by a 500-l/s turbomolecular pump associat-

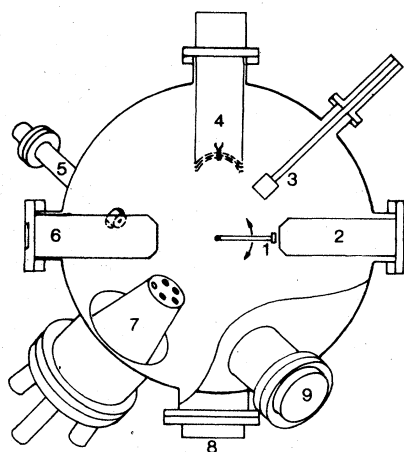


FIG. 1. Schematic diagram of the multiple technique apparatus to study interface formation. 1. Sample in a rotating arm. 2. Single-pass CMA used for Auger spectrometry. 3. Furnace. 4. LEED system. 5. RHEED electron gun. 6. Photoemission yield spectroscopy. 7. Set of five converging evaporation cells. 8. Viewport. 9. RHEED screen. The sample manipulator is on top of and the pumping system below the vacuum chamber.

ed with a liquid- N_2 -cooled titanium sublimation pump. Such a pumping system avoids the presence of spurious electric charges which would impair the photoemission yield measurements. The sample, 6×4 mm in section, is mounted 10 cm off the axis of a Varian manipulator and can be rotated and adjusted in different positions for each treatment or measurement.

The equipment for surface preparation includes the following: (i) a cleavage system made of an asymmetrical knife and a copper anvil which can be translated against the parallelepipedic sample with pre-cut notches, (ii) a small tantalum plus tungsten cylindrical furnace which allows surface annealing up to 1000°C with a negligible pressure rise, and (iii) a differentially pumped ion gun which has not been used in the present study.

Metal evaporations are made through a system such as those used for molecular beam epitaxy. A large flange can accommodate up to five evaporating cells, each one in an equivalent position at 15° of the flange main axis which itself is at 30° of incidence with respect to the surface under study: Thus, the extreme values of the metal beam angle of incidence on the sample surface are roughly 15° and 45° , depending on the position of the evaporation cell. Each cell is mounted into a cylinder which can be cooled either by water or liquid N_2 . In the present case where Ag films are formed, a graphite crucible of the Knudsen-type is used. The cell is thoroughly outgassed then calibrated in an auxiliary UHV system simulating the geometry of the main chamber. The evaporation rate is determined as follows. First, thick films are deposited on a glass substrate and staircaselike structures are prepared using a translatable screen: Interferential microscopy gives an absolute value of the film thickness in the range of a few thousand \AA . At the same time, a quartz balance is calibrated. Then the quartz balance is used to measure the low evaporation rates and to check their stability and reproducibility. Another quartz balance is mounted in the main chamber to periodically check the system. In the present experiments, an evaporation rate of 10^{-3} ML/s with an incident silver beam at 45° from the sample surface normal is used. However, neither an increase of the evaporation rate to 10^{-2} ML/s nor a change to a 15° incidence has been observed to have any influence on the results. During evaporation, the pressure increase in the chamber is negligible.

To study the surface properties, several techniques are available. For Auger measurements, a

single-pass Varian cylindrical mirror analyzer (CMA) with a coaxial electron gun is used. A Riber LEED optics is operated in a conventional mode and used to visually observe the diagram changes, Polaroid pictures being taken to keep track of the results. A RHEED system can be operated during film deposition but has not been used in the present experiments.

Photoemission yield measurements can also be performed in the photon energy range from 4 to 6.6 eV, from which the work function, the ionization energy, and the effective density of filled states in the gap and the upper part of the valence band of the semiconductor under study can be deduced. The principles of the measurement and of the data analysis have been described earlier.^{16,17}

In the present work, a set of oriented monocrystalline silicon bars has been studied, the free-carrier densities of which are, respectively, $n = 2.4 \times 10^{14} \text{ cm}^{-3}$, $n^+ = 2.5 \times 10^{19} \text{ cm}^{-3}$, and $p^+ = 1 \times 10^{19} \text{ cm}^{-3}$. The 2×1 reconstructed surface is obtained by cleavage along the $[\bar{2}11]$ direction in the (111) plane. The cleaved surface is never perfectly flat, and so shadowing effects can alter the homogeneity of the silver coverage. However, these effects are negligible since no change has been observed in the results upon varying the Ag beam incidence from 45° to 15° .

In a given experiment, the successive silver deposits and measurements are performed within at most 10 h after cleavage during which it has been checked the pressure never rises above 4×10^{-10} Torr. To avoid spurious effects due to ionized species, the vacuum gauge remains turned off during the experiments. Possible contamination effects will be discussed in the next sections.

III. RESULTS

A. Low-energy electron diffraction

After cleavage under ultrahigh vacuum, the clean (111) face of silicon is well known to give a LEED diagram corresponding to a 2×1 reconstructed surface. This has been observed in the present case as shown in Fig. 2(a) with sharp spots, weak background, and either a single domain or, more often, two domains.

Upon Ag deposition the 2×1 superstructure remains and a new structure starts to develop at a coverage of about 0.3 ML. Compared to the silicon (111) unit cell extrapolated from the bulk, this new structure is identified as a $(\sqrt{7} \times \sqrt{7})R 19.1^\circ$ with domains symmetrical about a (110) plane, and

the sharpest diagrams are obtained at a Ag coverage of about two-thirds of a monolayer. An example is shown in Fig. 2(b). The observation of an ordered silver layer in that coverage range after deposition at room temperature has not been reported previously. We have observed it each time even when some background, possibly due to cleavage defects, was blurring the LEED pattern. The same observation was made upon varying the incidence of the silver beam and the deposition rate, indicating this structure is not due to particular evaporation conditions.

Besides a loss of contrast in the diagrams, further silver deposition brings in new spots beyond 1 ML which superimpose onto the weakening 2×1 and $\sqrt{7} \times \sqrt{7}$ patterns. They correspond to the 1×1 structure of the silver (111) face. In fact, between about 1 and 2 ML of silver, the three sets of patterns can be observed together, as shown in Fig. 2(c). [For clarity, a schematic drawing of the three superimposed diagrams is shown in Fig. 2(d).] As Θ increases in this coverage range, the fractional order spots of the 2×1 and $\sqrt{7} \times \sqrt{7}$ superstructures become weaker and they are no longer observed at $\Theta \approx 2$ ML. At higher coverages, only Si(111) (1×1) and Ag(111) (1×1), with the same orientation are observed; the spot intensities of the former decreasing while those of the latter increase.

B. Auger electron spectroscopy

The variation of the peak-to-peak Auger signal of both silicon, at 91 V, and silver, at 350 V, versus silver coverage is shown in Fig. 3. The initial linear increase of the Ag peak is observed up to about 2 ML and there is no noticeable change of slope around 0.7 ML associated with the sharpest $\sqrt{7} \times \sqrt{7}$ superstructure. At $\Theta \approx 2$ ML where a change of slope is observed in the Ag signal, there are roughly 1.5×10^{15} Ag atoms per cm^2 on the silicon substrate, i.e., about the same density as in the (111) plane of bulk Ag metal. Beyond 10 ML average coverage, the Ag signal keeps on increasing and begins to saturate between 50 and 100 ML. On the other hand, the Si Auger signal decreases and the decrease becomes very slow at high coverages; the peak height reaches half its value after cleavage with 10 ML of Ag on the surface and has decreased by a factor of 5 at $\Theta = 100$ ML. The Auger observations are compatible with the homogeneous initial growth of a silver layer followed by the formation of large silver islands, growing both

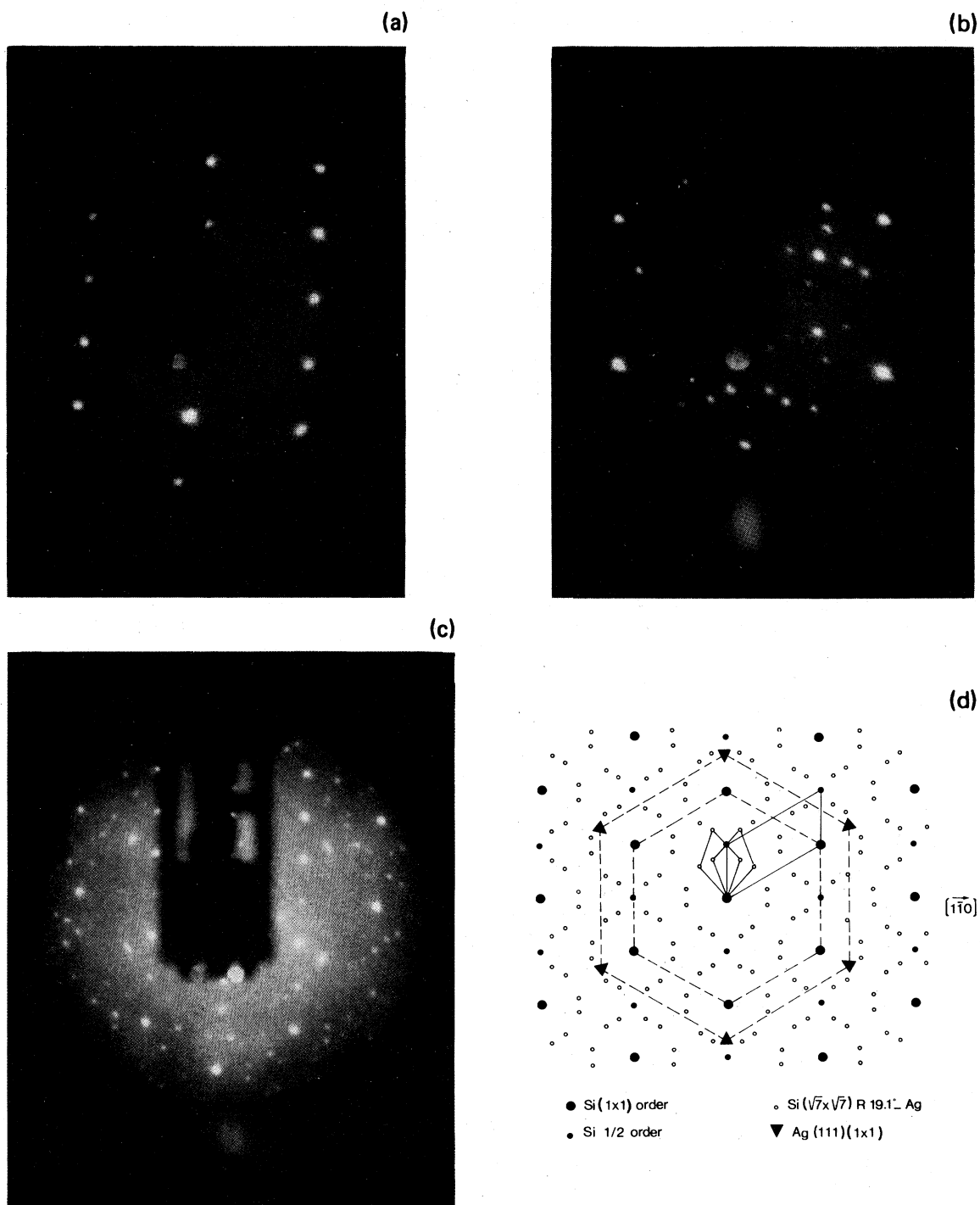


FIG. 2. LEED of the Si(111) $(2 \times 1) + \text{Ag}$ system for different silver coverage. (a) clean cleaved Si(111) surface. Electron primary energy $E_p = 70$ V; (b) Si(111) + 0.6 ML of Ag — $E_p = 46$ V; (c) Si(111) + 1.3 ML of Ag — $E_p = 125$ V; (d) Drawing of the superposed (2×1) Si(111), $\sqrt{7} \times \sqrt{7}$ Ag, and (1×1) Ag(111) diagrams.

in thickness and area on the surface. Clearly, from Auger measurements alone, other models of interface formation could be inferred; for example, the possibility of interdiffusion could be considered.

However, LEED and Auger electron spectroscopy (AES) results obtained when depositing Ag on a heated Si(111) substrate^{6,7} are explained without involving interdiffusion or, if any, within no more

than a double Si(111) atomic plane. It therefore seems reasonable in the present case, where Ag deposition is made on an unheated substrate, to look for a model where interdiffusion is not involved.

Auger measurements were also made to check the sample surface contamination. No trace of contaminant besides carbon and oxygen could be found within the sensitivity of the system. The presence of some carbon together with silver cannot be excluded. However, any quantitative evaluation is difficult since the carbon peak, at 271 V, is very close to the satellite peak of silver at 270 V. An upper limit of a few percent of a monolayer can only be proposed. The presence of an oxygen peak at 507 V is observed at the end of the experiments. An evaluation of the oxygen concentration is possible from the measurement of the signal at monolayer coverage, which is roughly obtained after exposure of a clean cleaved surface to a few thousand Langmuirs of oxygen. It shows that, in the worst cases at the end of a long experiment, the total oxygen coverage is always below 0.08 ML. Even then, the influence of oxygen contamination on the LEED and photoemission results appears negligible.

C. Photoemission yield spectroscopy

The results are presented in terms of the effective density of filled states $N^*(E)$ as deduced from the measured photoemission yield spectra by taking the first derivative with respect to photon energy.^{16,17} In Fig. 4, the successive $N^*(E)$ obtained at increasing silver coverages are shown in the case of a

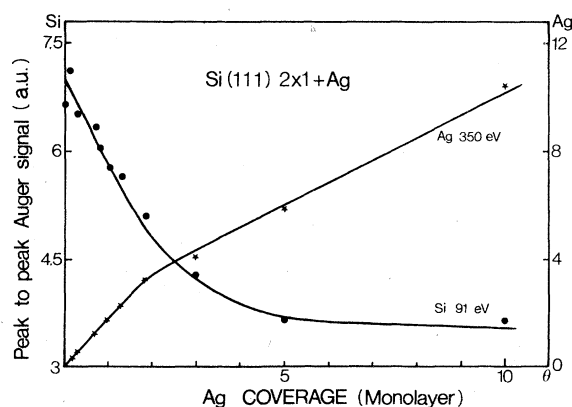


FIG. 3. Peak-to-peak Auger signal for Si and Ag versus silver coverage. $E_p = 2$ kV, $I_p = 5 \mu\text{A}$, modulation voltage = 5 V peak to peak.

lightly doped silicon sample. In this case, the escape length of electrons is small compared to the depth of the space-charge region, therefore there is no observable band bending effect, but the Fermi level is at its surface position with respect to the bands. Both the semilog plots and the linear plots are presented to show the behavior of the curves, respectively, at low and high photon energy in the covered range.

The value of the work function ϕ is obtained by fitting the low-energy tail of the effective density of filled states, shown in the semilog plot of Fig. 4, with the Fermi distribution function. This procedure is accurate within about 50 MeV in the present case where the density of states in the gap is not too low; it gives an absolute value of the work function of the clean cleaved silicon surface in excellent agreement with the accepted value. The variation of ϕ upon silver coverage Θ , which is given in Fig. 5, is even more accurately determined because the shape of the low-energy tail of $N^*(E)$ remains almost unchanged when Θ increases. The variation of the ionization energy Φ is also shown in Fig. 5. The value of Φ for the clean surface is deduced from the results obtained on differently doped samples.^{16,17} The same procedure has been followed to determine Φ at different silver coverages. However, the ionization energy variations can also be obtained directly in

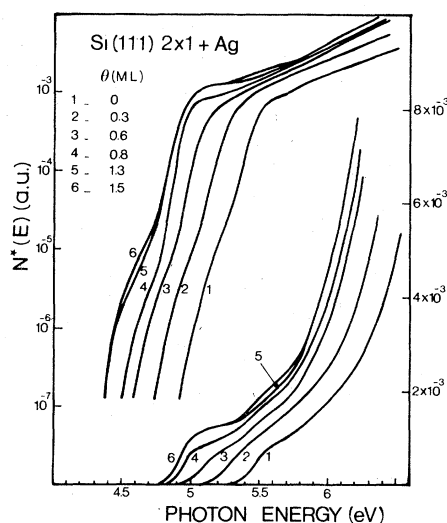


FIG. 4. First derivative of the photoemission yield with respect to photon energy, called effective density of filled states (see text), versus photon energy for a lightly doped cleaved silicon sample at different silver coverages. Both semilog (left scale) and linear (right scale) plots of the same curves are presented.

Fig. 4 by measuring the energy amount by which a given curve must be translated to make it coincide with curve 1 in the region where Si bulk states dominate, for example, along a line at $N^*(E) = 5 \times 10^{-3}$ scale unit. Both methods give similar values.

Figure 4 also contains all the information about the Ag-induced changes in the density of filled states. Thus, it is clearly visible that, between curves 5 and 6, $N^*(E)$ has increased close to the Fermi level and at about 1.1 eV below it. However, variations occurring close to the top of the silicon valence band E_v are made more visible by (i) taking E_v as the origin of the energy and (ii) removing the contribution of the silicon bulk states. The first point is obtained by taking into account the ionization energy changes. The second point can be approximately satisfied by subtracting from each curve, once translated, the same contribution which follows a law of the form $(E - \epsilon)^m$ and has been fitted, between 6.3 and 6.5 eV, to the $N^*(E)$ curve obtained immediately after cleavage (the best fit is observed for $m = \frac{5}{2}$ and $\epsilon = 5.35$ eV). The results are shown in Fig. 6. To check the significance of this representation, the curve corresponding to the clean surface has been compared to the difference between the effective densities of states of the clean cleaved surface and of the same surface after an oxygen exposure just sufficient to remove the dangling-bond surface states. It appears that there is no significant difference between the two results. Therefore, keeping in mind how the representation has been obtained, the quantity shown in Fig. 6 will be called an effective density of surface states $N_s^*(E)$.

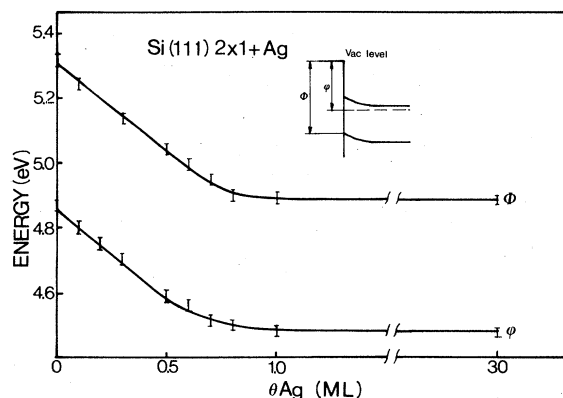


FIG. 5. Variations of the work function ϕ and ionization energy Φ of the system cleaved Si(111)+Ag versus silver coverage.

IV. DISCUSSION

At low silver coverages during the initial stage of the Si-Ag interface formation, the following observations are made: in LEED, a $\sqrt{7} \times \sqrt{7}$ superstructure is observed, superimposed onto the 2×1 substrate superstructure; in Auger, the Ag peak increases linearly with Θ while the Si signal shows a linear decrease; and the work function decreases linearly with coverage. This linear variation of ϕ with Θ indicates the deposited silver does not cluster in metallic islands. Otherwise, the low work function areas would impose a sharp threshold decrease at low coverage. The above observations are compatible with the formation of an ordered silver layer.

On the other hand, at high coverages the Ag(111) (1×1) structure is observed together with a weak Si(111) (1×1) in Auger, the Ag signal keeps on increasing but the Si peak becomes constant; and the work function remains constant at about 4.5 eV. Now, the deposited silver forms metallic islands imposing the value of ϕ but enabling the observation of Si in LEED and Auger at very large coverages.

Therefore, the room-temperature formation of the interface between silver and the clean cleaved 2×1 reconstructed Si(111) surface appears to occur in two successive steps. The first step is the formation of an ordered silver layer which is completed at a coverage Θ_1 between half and full mono-

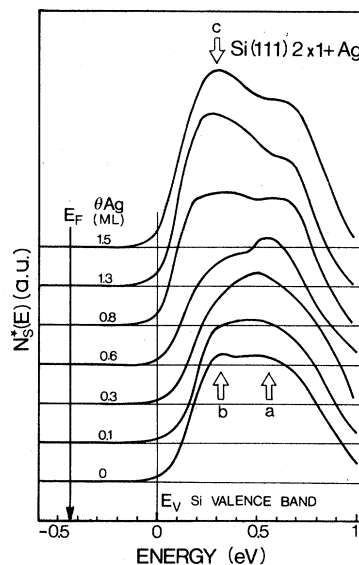


FIG. 6. Changes in the effective density of surface states $N_s^*(E)$ as defined in the text, for the system cleaved Si(111)+Ag upon increasing silver coverage.

layer. The second part of the interface formation is the growth of oriented crystalline Ag islands; the (111) plane of silver is parallel to the Si(111) plane with the same in-plane orientation.

It is difficult to propose an accurate value for Θ_1 since (i) the absolute value of the average silver coverage, without considering the fluctuations along a cleaved surface, is known with about 15% accuracy, and (ii) neither LEED nor Auger nor photoemission give a clear-cut change upon completion of the initial layer. The sharpest indication of Θ_1 is given in Fig. 5 by the coverage at which both the work function and ionization energy have stopped to decrease, provided the initial silver layer has to be completed before the second growth process starts. Finally, any number from 0.6 to 0.8 ML would be acceptable.

The observation of the $\sqrt{7} \times \sqrt{7}$ superstructure at room temperature implies the silver atoms can move sufficiently along the surface and interact with one another to form a low-density ordered overlayer with an average distance between silver atoms of about 4.7 Å which is much larger than the nearest-neighbor distance of 2.9 Å in Ag metal. Thus the silver atoms do not interact strongly with silicon.

The weak interaction between Si and Ag inferred from the LEED observations is consistent with the electronic properties. Indeed, the ionization energy varies like the work function of the system, which means there is no significant change of the band bending upon increasing silver coverage. Variations of both Φ and φ are simply explained by a decrease of the vacuum level energy. It implies also that the density of states localized at the interface must remain practically the same as on the clean surface, at least within the gap. This is exactly what is actually observed in Fig. 4, where on the semilog plot the tail of occupied surface states in the gap is simply translated without any deformation with increasing silver coverage, up to Θ_1 . Then upon metallic silver formation, new states appear at the Fermi level but they do not influence the already stabilized interface. Therefore, since the tail of surface states within the gap of silicon is

a part of the dangling-bond surface-state band of the clean cleaved surface, this band should not be removed by the silver layer. Figure 6 shows clearly that the surface-state band at zero coverage, with its main part labeled "a" and its step-induced part labeled "b", remains roughly unchanged up to Θ_1 Ag coverage. The only effect is apparently the removal of the step-induced peak "b". It shows that the dangling bonds behave as if they were unaffected by the presence of silver atoms. Upon further silver deposition, a new peak labeled "c" in Fig. 6 grows roughly at the same energy as the step-induced peak b. However, as in the gap, these states are simply added to the silicon surface states and do not change the electronic properties of the interface. Therefore, even at high silver coverages, the peak attributed to the dangling bond remains present. Since it governs the Fermi-level position at the silicon surface, the Schottky barrier which is formed must be such that no band bending change occurs. The measurements performed earlier elsewhere^{14,15} confirm this conclusion.

It would be interesting to know the arrangement of silver atoms in the first layer at the interface. The uncertainty in the absolute coverage when the first layer is complete prevents us from proposing any specific model of structure. However, the persistence of the dangling-bond peak seems to indicate that a model with a silver atom on top of more than about ten percent of the silicon surface atoms is very unlikely.

In summary the Si(111) (2×1)-Ag interface formed at room temperature is made of a dilute ordered silver layer which separates the silicon crystal from the metallic silver crystal and keeps almost unchanged the electronic properties of the clean cleaved silicon surface.

ACKNOWLEDGMENTS

The technical assistance of B. Helie is gratefully acknowledged. This work was supported in part by Centre National de la Recherche Scientifique under Contract No. ATP 3834.

*On leave from Conservatoire National des Arts et Métiers, France.

† On leave from University of Fudan, Shanghai, People's Republic of China.

¹See, for example, *Handbook on Semiconductors*, edited

by T.S. Moss and M. Balkanski (North-Holland, Amsterdam, 1980), Vol. 2, Chap. 3.

²E. Bauer and H. Poppa, *Thin Solid Films* **12**, 167 (1972).

³G. Le Lay, Ph.D. thesis, University of Marseille III,

- 1977 (unpublished).
- ⁴K. Spiegel, Surf. Sci. 7, 125 (1967).
- ⁵G. Le Lay, G. Quentel, J. P. Faurie, and A. Masson, Thin Solid Films 35, 273 (1976); 35, 283 (1976).
- ⁶G. Le Lay, N. Manneville, and R. Kern, Surf. Sci. 72, 405 (1978).
- ⁷F. Wehking, H. Beckermann, and R. Niedermayer, Surf. Sci. 71, 364 (1978).
- ⁸M. Housley, R. Heckingbottom, and C. J. Todd, Surf. Sci. 68, 179 (1977).
- ⁹S. Ino and Y. Gotoh, Jpn. J. Appl. Phys. 16, 2261 (1977).
- ¹⁰Y. Gotoh and S. Ino, Jpn. J. Appl. Phys. 17, 2097 (1978).
- ¹¹J. Derrien, G. Le Lay, and F. Salvan, J. Phys. (Paris) Lett. 39, L287 (1978).
- ¹²J. P. Gaspard, J. Derrien, A. Cros, and F. Salvan, Surf. Sci. 99, 183 (1980).
- ¹³A. McKinley, R. H. Williams, and A. W. Parke, J. Phys. C 12, 2447 (1979).
- ¹⁴A. Thanailakis, J. Phys. C 8, 655 (1975).
- ¹⁵J. D. Van Otterloo and J. G. De Groot, Surf. Sci. 57, 93 (1976).
- ¹⁶C. A. Sebenne, D. Bolmont, G. M. Guichar, and M. Balkanski, Phys. Rev. B 12, 3280 (1975).
- ¹⁷C. A. Sebenne, Nuovo Cimento 39B, 768 (1977).

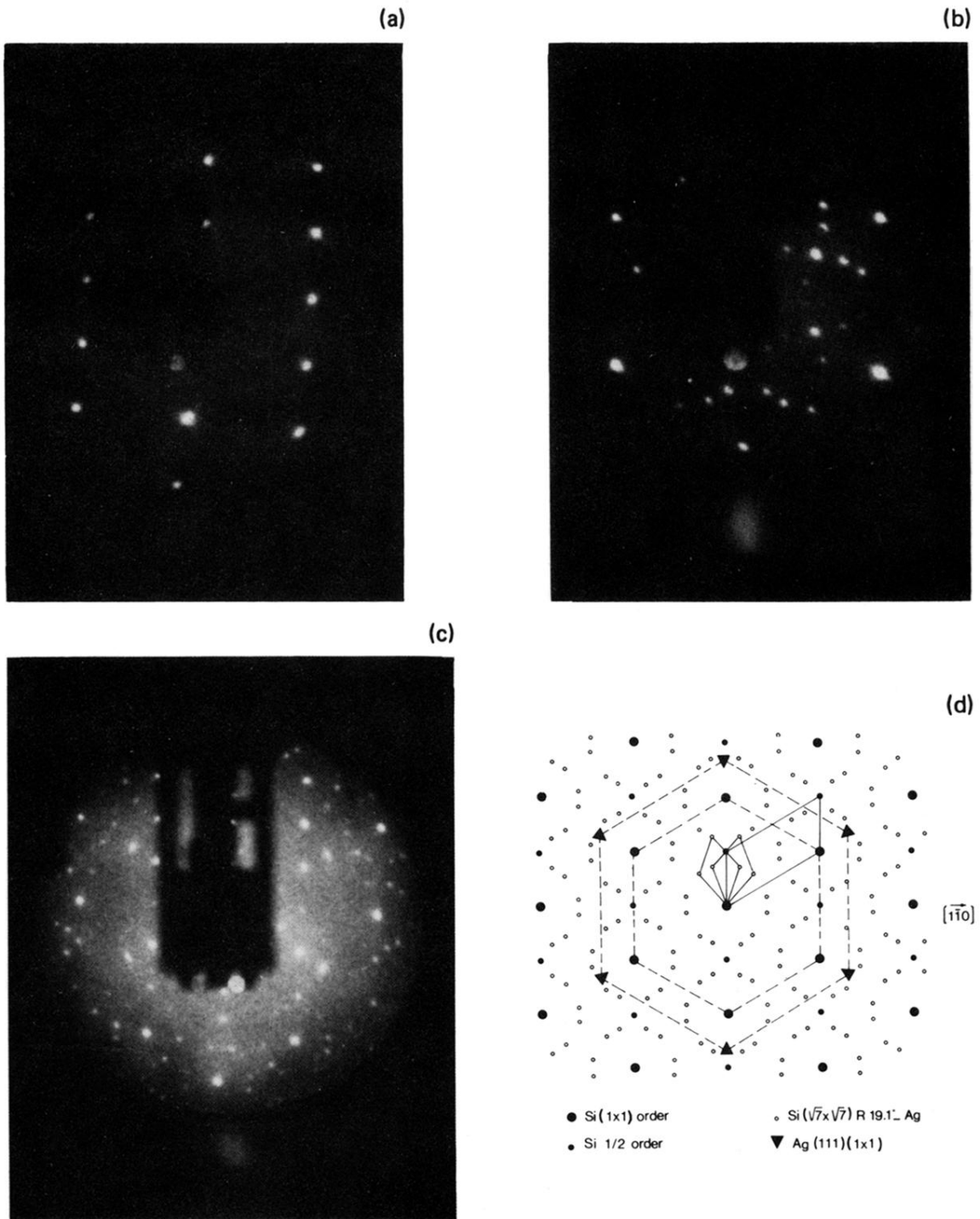


FIG. 2. LEED of the Si(111) (2×1) + Ag system for different silver coverage. (a) clean cleaved Si(111) surface. Electron primary energy $E_p = 70$ V; (b) Si(111) + 0.6 ML of Ag — $E_p = 46$ V; (c) Si(111) + 1.3 ML of Ag — $E_p = 125$ V; (d) Drawing of the superposed (2×1) Si(111), $\sqrt{7}\times\sqrt{7}$ Ag, and (1×1) Ag(111) diagrams.